Human Molecular Genetics, 2005, Vol. 14, No. 21 ***3161–3168***
doi:10.1093/hmg/ddi348
Advance Access published on September 13, 2005

Dominant mutations of Col4a1 result in basement membrane defects which lead to anterior segment dysgenesis and glomerulopathy

Tom Van Agtmael[1,3,*], Ursula Schlötzer-Schrehardt[4], Lisa McKie[3], David G. Brownstein[2], Angela W. Lee[3], Sally H. Cross[3], Yoshikazu Sado[6], John J. Mullins[1], Ernst Pöschl[5] and Ian J. Jackson[3]

[1]Molecular Physiology, Centre for Cardiovascular Science and [2]Division of Pathology, School of Molecular and Clinical Medicine, University of Edinburgh, 47 Little France Crescent, Edinburgh EH16 4TJ, UK, [3]Medical Research Council Human Genetics Unit, Crewe Road, Edinburgh EH4 2XU, UK, [4]Department of Ophthalmology and [5]Department of Experimental Medicine I, University of Erlangen-Nürnberg, Germany and [6]Shigei Medical Research Institute, Okayama, Japan

Received May 6, 2005; Revised July 4, 2005; Accepted September 8, 2005

Members of the type IV collagen family are essential components of all basement membranes (BMs) and define structural stability as well as tissue-specific functions. The major isoform, α1.α1.α2(IV), contributes to the formation of many BMs and its deficiency causes embryonic lethality in mouse. We have identified an allelic series of three ENU induced dominant mouse mutants with missense mutations in the gene *Col4a1* encoding the α1(IV) subunit chain. Two severe alleles (*Bru* and *Svc*) have mutations affecting the conserved glycine residues in the Gly-Xaa-Yaa collagen repeat. *Bru* heterozygous mice display defects similar to Axenfeld–Rieger anomaly, including iris defects, corneal opacity, vacuolar cataracts, significant iris/corneal adhesions, buphthalmos and optic nerve cupping, a sign indicative of glaucoma. Kidneys of *Bru* mice have peripheral glomerulopathy characterized by hypertrophy and hyperplasia of the parietal epithelium of Bowman's capsule. A milder allele (*Raw*) contains a mutation in the Yaa residue of the collagen repeat and was identified by a silvery appearance of the retinal arterioles. All phenotypes are associated with BM defects that affect the eye, kidney and other tissues. This allelic series shows that mutations affecting the collagen domain cause dominant negative effects on the expression and function of the major collagen IV isoform α1(IV), and pathological effects vary with the individual mutations.

INTRODUCTION

Anterior segment dysgenesis (ASD) is a collection of disorders that affect the anterior eye structures, iris, lens, cornea and drainage networks, and includes Axenfeld's, Rieger's and Peter's anomalies, aniridia, iridogoniodysgenesis and posterior embryotoxon (1). Axenfeld–Rieger (AR) anomaly is characterized by iridocorneal adhesions, corneal opaqueness and various iris defects including tears, hypoplasia and eccentric pupil. Importantly, 50% of AR patients develop glaucoma (2). AR is genetically heterogeneous, and some causative genes have been identified, including *PITX2* and *FOXC1* (3–6). However, linkage of AR to other loci (reviewed in 2) and the absence of mutations in known ASD genes in patients (reviewed in 1) indicate that multiple genes underlie AR. The genetic heterogeneity of ASD is paralleled by inter- and intra-familial phenotypic variability (1).

Mouse models are an excellent tool to analyse gene function, and ENU (*N*-ethyl-*N*-nitrosourea) mutagenesis generates single base pair changes that can accurately model human disease-causing mutations (7). As a part of an ENU mutagenesis project for dominant eye phenotypes, we identified two

*To whom correspondence should be addressed at: Molecular Physiology, Centre for Cardiovascular Science, University of Edinburgh, 47 Little France Crescent, Edinburgh EH16 4TJ, UK. Email: tom.vanagtmael@ed.ac.uk

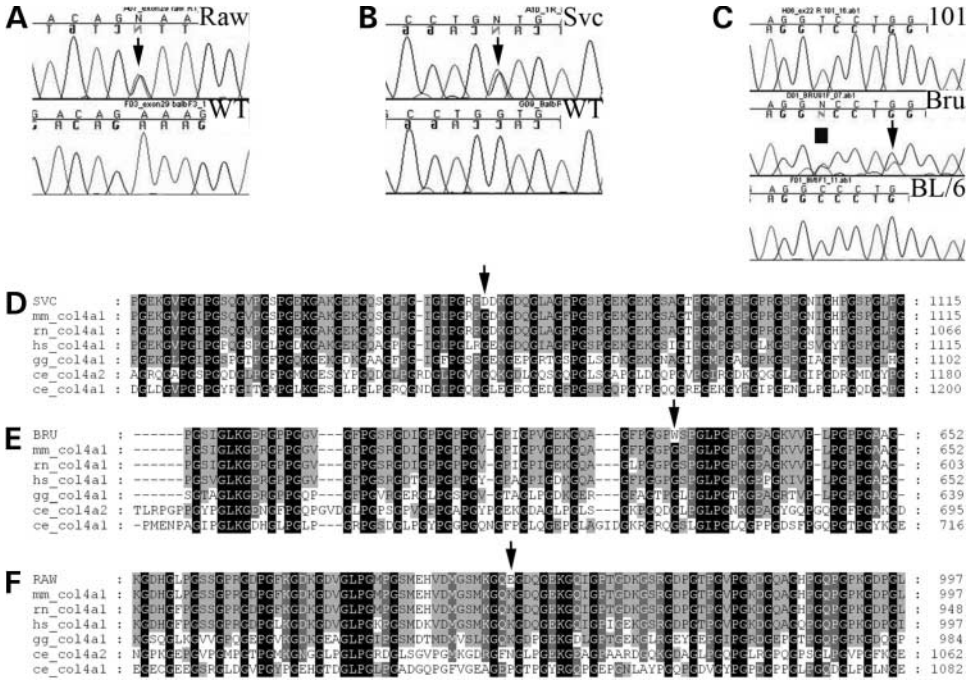

Figure 1. *Raw*, *Svc* and *Bru* are caused by mutations in the gene *Col4a1*. (**A**) Sequence analysis of *Col4a1* exons identified a G-A mutation in *Raw* (arrow). (**B** and **C**) Sequence analysis of *Svc* (B) and *Bru* (C) identified an A-G and G-T mutation, respectively (arrow). The sequence trace also shows a polymorphism (square) in *Bru* between the two background strains 101 and C57BL/6. (**D**) In *Svc*, a highly conserved glycine residue has been replaced by an aspartic acid (G1064D) (arrow). (**E**) *Bru* mice have a glycine to tryptophan mutation (G627W) (arrow). (**F**) The mutation in *Raw* substitutes a lysine residue by glutamic acid (K950E) (arrow). The lysine residue is conserved in vertebrates, whereas it does not seem to be conserved in *C. elegans*. Mm, hs, rn, gg and ce indicates *Mus musculus*, *Homo sapiens*, *Rattus norvegicus*, *Gallus gallus* and *C. elegans*, respectively. *C. elegans* Col4a1 sequence is from EMB-9 and Col4a2 is LET-2 sequence (22). (The amino acid numbering is based on NCBI Col4a1 Seq. accession no. NP_034061.)

mutants, *Raw* (retinal arteriolar wiring) and *Svc* (small with vacuolar cataracts), with overlapping eye phenotypes (8). *Raw* displays a silvery appearance of the retinal arterioles and *Svc* has vacuolar cataracts, small body size, bruising at birth and some arteriolar silvering (See Figure 2 in 8).

Interestingly, both *Raw* and *Svc* co-localize in a 10 Mb region on chromosome 8 between markers *D8Mit124* and *D8Mit155*. This was coincident with the location of a third mutant, *Bruised* (*Bru*) (9). *Bru* homozygous mice are embryonic lethal, and heterozygotes have a phenotype similar to *Svc*, including bruising at birth, small body size and various eye defects (10). Although *Bru* was found among the offspring of an ENU-mutagenized male, it was reported to be caused by a visible deletion of cytogenetic band A1.3 of chromosome 8 (9). The overlapping phenotypic features and mapping data suggested that these mutants may be allelic (8).

We show here that three mouse mutants, *Raw*, *Bru* and *Svc*, are an allelic series due to point mutations in the gene *Col4a1*. These mutations result in glomerulopathy and symptoms similar to defects seen in AR anomaly. The observed phenotypes are associated with generalized basement membrane (BM) defects but show a high degree of tissue-specific variability. A genotype–phenotype correlation exists, as mutations affecting the crucial glycine residues in the Gly-Xaa-Yaa repeat result in more severe pathologies. These mutations define a spectrum of diseases caused by mutations of the major collagen IV isoform.

RESULTS

Bru, *Raw* and *Svc* are caused by *Col4a1* mutations

Bru was reported to be caused by a deletion of cytogenetic band A1.3 on chromosome 8 (9), which is contained in the *Raw* and *Svc* candidate region between *D8Mit124* and *D8Mit155* (8). To determine the extent of any deletion, offspring from *Bru* and M.m. castaneus inter-cross matings were genotyped using microsatellites spanning the *Raw* and *Svc* candidate region (*D8Mit149*, *D8Mit333*, *D8Mit157*, *D8Mit285*, *D8Mit173*, *D8Mit141* and *D8Mit60*). Offspring carrying the *Bru* chromosome had heterozygous genotypes for all markers, indicating that *Bru* was not caused by a large deletion (data not shown). A genome scan was therefore undertaken which mapped the *Bru* mutation proximal of D8Mit259 on chromosome 8 ($\chi^2 = 6.23$, one degree of freedom, P-value < 0.05).

The co-localization of the *Bru* and *Raw*/*Svc* candidate regions and overlapping phenotypes suggested that the mutations may be allelic. Further mapping reduced the *Raw*/*Svc* candidate region to a 7 Mb interval between SNP WI_WGS_8_6825671 (http://www.jax.org/phenome) and *D8Mit60*. Owing to the absence of additional informative markers, we performed candidate gene sequence analysis. Examination of *Col4a1*, which encodes the α1 chain of type IV collagen, α1(IV), identified missense mutations in all three alleles. For *Raw* mice, a mutation was detected in exon 34 (Fig. 1A) whereas in *Svc* and *Bru*, we detected a base pair

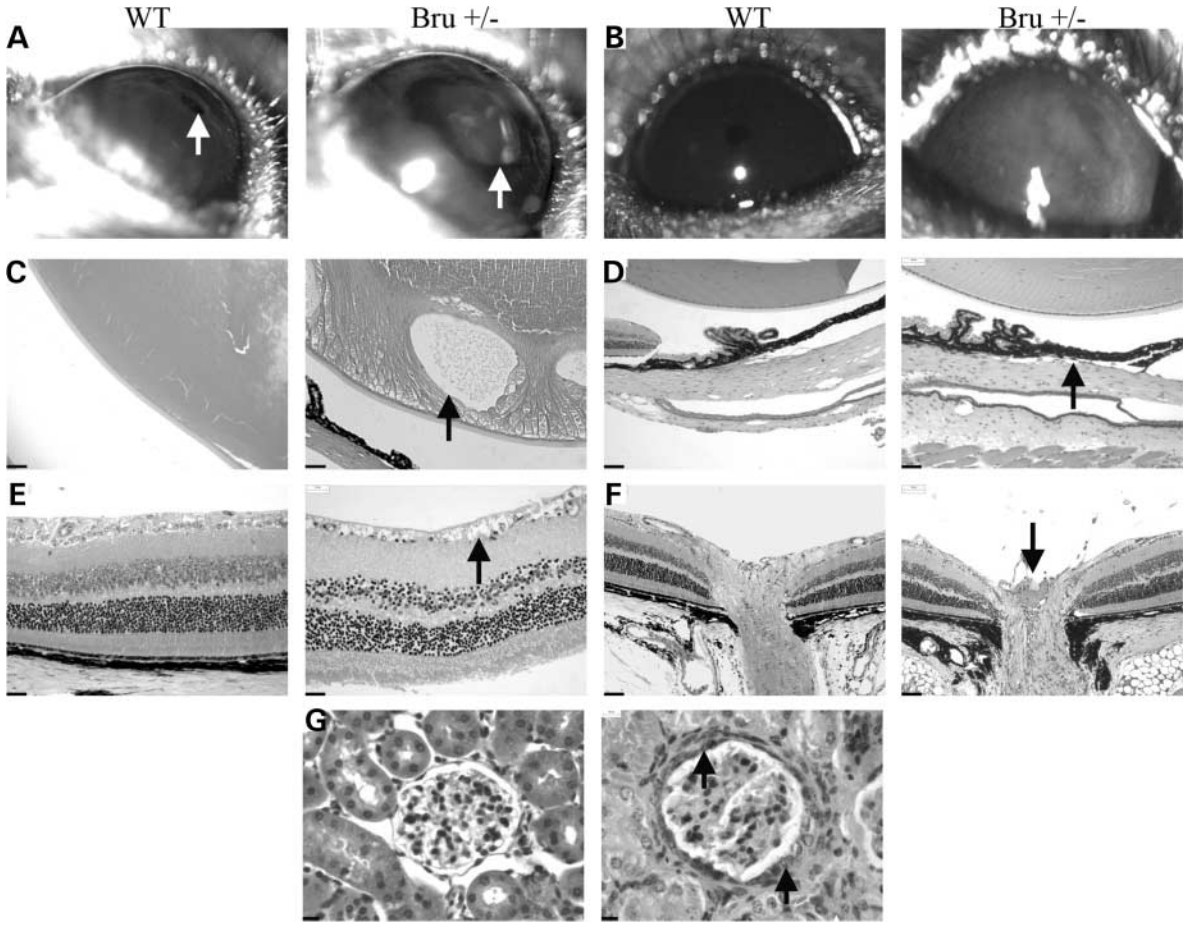

Figure 2. (**A**) *Bru* animals have buphthalmos, abnormal pupil which fails to constrict upon light stimulation (arrow), (**B**) corneal opacity, (**C**) vacuolar cataracts (arrow), (**D**) iris/corneal adhesion (arrow), (**E**) degeneration of the ganglion cell layer (arrow) and (**F**) optic nerve cupping (arrow). (**G**) In *Bru*, the glomeruli have irregular linings of parietal epithelium of Bowman's capsule (arrow). Hyperplastic nuclei are clustered in interrupted rows of three or more with intervening gaps. The peri-glomerular interstitium has an increased cellularity in cells with fusiform nuclei consistent with fibroblasts. Scale bar: (C, D and F) 50 μm; (E) 25 μm; (G) 10 μm.

change in exons 37 and 26, respectively (Fig. 2B and C). All base pair changes segregated with their respective phenotypes and were absent in a panel of wild-type (WT) laboratory strains, including the strains of origin (BALB/c for *Raw* and *Svc* and C3H/101 for *Bru*). Sequence analysis of α1(IV) cDNA from *Raw* and *Bru* showed the presence of both mutant and WT alleles, indicating that the mutant alleles are expressed and suggesting that mutant proteins may be produced (data not shown).

All mutations are located in the central collagen domain of α1(IV) which consists of multiple Gly-Xaa-Yaa repeats separated by short interruptions of non-collagenous sequences. All three mutations affect residues of the Gly-Xaa-Yaa repeat. In *Svc* and *Bru*, the mutations substitute the critical glycine residues for an aspartic acid (G1064D) and tryptophan (G627W) residue, respectively (Fig. 2D and E). Both these amino acid changes are predicted to result in severe detrimental effects on collagen triple helix formation and stability. Although the *Svc* mutation is located in the most 3′-terminal homogenous collagenous domain, the *Bru* mutation is located centrally in a short collagenous domain flanked by interruptions and may disturb the folding of this domain. In contrast, the *Raw* (K950E) mutation causes a positively charged lysine residue, located at the Yaa position, to be replaced by a negatively charged glutamic acid. Comparative sequence analysis shows that this lysine residue is conserved throughout evolution in vertebrates (Fig. 1F). As this mutation is located in the first Gly-Xaa-Yaa repeat following a major interruption, it may affect the structure at this highly flexible site. The correlation of an allelic series of mutants with the base pair changes in *Col4a1* indicates that these mutations are causative of the described phenotypes.

Mutations in Col4a1 result in ASD

Signs of ASD are apparent in *Bru* mice at or shortly after weaning. By 3 months, half of the *Bru* eyes (8/16) display buphthalmos (bulging eyes) (Fig. 2A), a possible sign of glaucoma, and ∼20% of the eyes display corneal opacity (3/16) (Fig. 2B). Additionally, some animals have malformed pupils, which fail to constrict on light stimulation (Fig. 2A). Histopathological analysis on 3-month-old mutant animals

showed that *Bru* eyes can have vacuolar cataracts (2/7 animals), retinal detachment (4/7 animals) and peripheral iridocorneal adhesion (anterior synechiae) (5/7 animals) (Fig. 2C and D). The adhesions may result in glaucoma by preventing proper drainage of the aqueous humour, leading to aqueous accumulation and possibly increased intra-ocular pressure (11). This may be the cause of the observed atrophy of the ganglion cell layer (3/7 animals) and cupping of the optic disc (3/7 animals) (Fig. 2E and F), a sign suggestive of glaucoma. No obvious defects were observed in *Raw* eyes, which could explain the arteriolar silvering (data not shown).

As mutations in other collagen IV genes, *COL4A3*-*COL4A5*, result in kidney defects characteristic of Alport syndrome (AS) (12), the kidneys of *Raw* and *Bru* mice were examined histopathologically. *Raw* kidneys did not display any clear defects (data not shown). In contrast, *Bru* kidneys have proliferation and hypertrophy of the parietal epithelial lining of Bowman's capsule (Fig. 2G). These defects are seen in both sexes. Affected glomeruli have irregular linings of parietal epithelium due to variations in cell size and nuclear density. In severe cases, multiple layers of parietal epithelium are present (data not shown). Changes in parietal epithelium are accompanied by increased numbers of fusiform cells consistent with fibroblasts in peri-glomerular interstitium.

To test whether the defects result in proteinuria, urine was collected from 5- to 6-month-old *Bru* and *Raw* mice; its protein content was quantified by Bradford assay and its composition was analysed by SDS–PAGE. No significant difference in protein content or composition was observed between the WT and mutants (data not shown).

Mutations in *Col4a1* result in variable tissue-specific BM defects

Collagen IV is an abundant component of all BM and is critical for the formation of stable BMs during embryonic development (13), but the specific expression of isoforms defines the characteristic properties of individual BMs. To further determine the causative defects of the observed phenotypes, the membranes of several tissues, including eye and kidney, were analysed in *Bru* and *Raw* mice by electron microscopy. In general mutants show variable changes in the thickness and appearance of BMs, and also local disruptions and detachment of matrix from cells can be observed.

The BM of the corneal epithelium is more severely affected in *Bru* animals, which display local interruptions, when compared with *Raw* in which the BM is continuous but less dense than in WT. (Fig. 3A). The lens capsule shows an irregular appearance in *Bru* when compared with the homogenous amorphous structure seen in *Raw* and WT lenses. In *Bru* mutants, a dilation of the vesicles from the endoplasmic reticulum (ER) of the lens epithelial cells can be observed (Fig. 3B). The BMs of the pigmented and non-pigmented epithelia of the ciliary body and iris in both *Raw* and *Bru* are locally disrupted or detached from the epithelial cells (Fig. 3C). It may be that these epithelial defects are responsible for the observed iridocorneal adhesion.

In general, the BM is more affected in *Bru* than in *Raw*, which correlates with the more severe histological changes. Typically, in epithelial BMs of the cornea in both *Raw* and *Bru*, almost normal BMs are found closely associated with hemidesmosomes. The interspace BMs of both mutants are less dense or even missing in *Bru*. This effect is also seen in the epithelium of the oesophagus (data not shown).

The vascular BMs surrounding the pericytes and endothelial cells of the retinal vessels are affected in both *Raw* and *Bru* mutants, displaying locally reduced thickness as well as focal interruptions (Fig. 3D). As no other histopathological phenotype was observed in *Raw* vessels, these changes may be linked with the observed arteriolar silvering seen by ophthalmoscope examination.

The inner limiting membrane (ILM) which covers the retina appears normal in most regions in *Raw* and *Bru*. Interestingly, local interruptions are observed in *Bru* (Fig. 3E), which can be accompanied by invasion of Mueller cell processes into the vitreous body. This may reflect the histological observation of fibro-vascular tufts in some *Bru* mice (10).

Analysis of the BMs of the kidney revealed no obvious defects in *Raw* mice. In *Bru*, the glomerular basal membrane (GBM) appears to be normal (Fig. 3F). However, in some areas, the endothelium underlying the GBM is locally degenerated, indicating a possible polarized pathological effect on these cells (data not shown). The tubular BMs of *Bru* mice were indistinguishable from normal BMs. However, Bowman's capsule is severely affected. Rather than a continuous, dense linear structure, the BM shows variable thickness, folding and local splitting into multiple layers (Fig. 3G). These results indicate that changes in the BM of Bowman's capsule may be the primary defect and determine the histopathological phenotype of *Bru* kidneys.

Mutations in *Col4a1* do not influence expression of other collagen IV isoforms

During kidney organogenesis, a developmental switch reduces expression of α1(IV) and α2(IV) and activates the expression of α3(IV)–α5(IV), which are crucial for the mature GBM (14). In AS patients, the mutations result in a loss of a functional α3.α4.α5(IV) network and alter the expression of α1(IV) and α2(IV), whereby the expression of the α1.α1.α2(IV) network is maintained and partially compensates for the loss of the α3.α4.α5(IV) network (12).

Quantitative RT–PCR analysis on cDNA from adult eyes of *Bru* and *Raw* animals did not reveal any significant changes in the mRNA expression of the other collagen IV isoforms (data not shown). However, collagen type IV is subject to post- transcriptional modification and regulation, which could alter the protein levels of the different collagen IV isoforms (15). To investigate whether mutations in *Col4a1* lead to differences in protein expression, we performed immunohistochemistry on WT, *Raw* and *Bru* eye sections using collagen IV chain-specific monoclonal antibodies (16). No significant differences in distribution could be observed in the different mutants (data not shown). We conclude that no obvious changes in collagen IV mRNA and protein expression occur to compensate for the effects of mutant α1(IV).

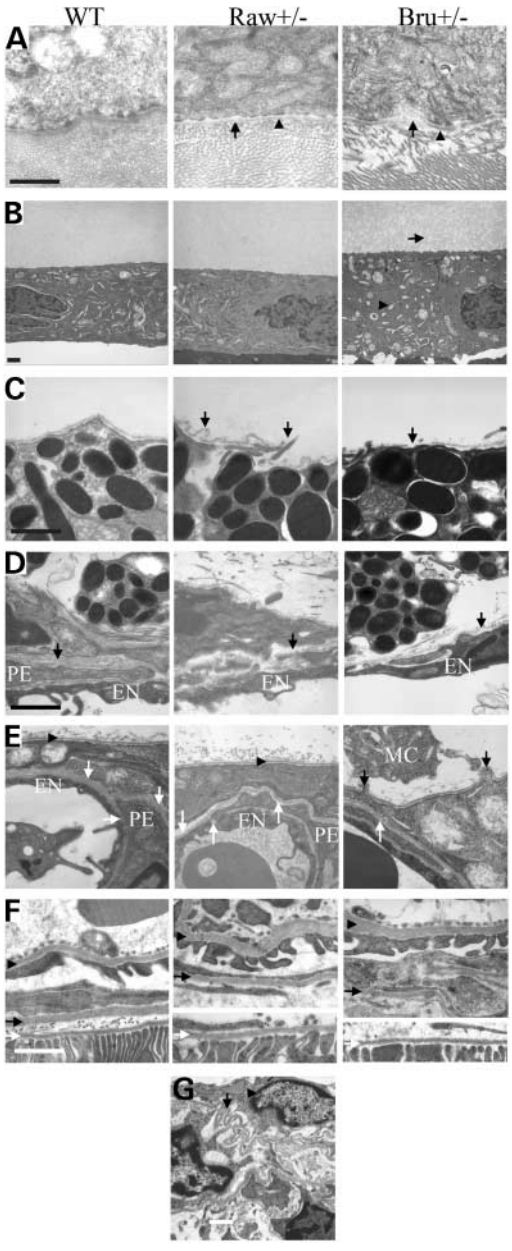

Figure 3. Ultrastructural analysis in both *Bru* and *Raw* identified local disruptions in the BMs in a variety of tissues. (**A**) The corneal epithelium of *Raw* is continuous but has areas in which the BM is less dense (arrow). In *Bru*, the BM can show interruptions (arrow). At hemidesmosomes (arrowhead), the BM appears normal in *Raw* and *Bru*. (**B**) The *Bru* lens capsule (arrow) appears irregular with a granular structure when compared with WT and *Raw* and a dilation of the ER can be observed (arrowhead). (**C**) The epithelial BM of the iris pigment epithelium has local disruptions and folds (black arrow) in both *Raw* and *Bru*. (**D**) The BM surrounding pericytes (PE) and endothelium (EN) of capillaries in the iris stroma (arrow) in *Raw* and *Bru* is fuzzier, less dense and has local interruptions. (**E**) In *Bru*, the ILM (arrowhead) covering the retina has local disruptions (arrow) which can lead to ectopia of Mueller cells (MC). The BM of the arterioles is thinner and has local disruptions (white arrow). The ILM in *Raw* is indistinguishable from WT. (**F**) The tubular BM (white arrow) and GBM (arrowhead) are mostly unaffected in *Raw* and *Bru*. Bowman's capsule in *Raw* is unaffected (arrow) but shows a number of defects in *Bru*. (**G**) A different region of section 3F in *Bru* animals shows splitting and the formation of folds (arrow) in the BM of Bowman's capsule in *Bru*. The epithelial cells have a hypertrophic appearance (arrowhead). Scale bar: (A and C–G) 1 μm; (B) 2 μm.

DISCUSSION

BMs are complex aggregates of matrix components, and differences between composition and interactions underlie the diversity of individual membranes. Collagen type IV, the major structural component of BMs (17), is crucial for its normal functioning, although not for its initial formation during embryonic development (13). Six different alpha chains belong to the family of the type IV collagen molecules which can form three distinguishable networks (12). Mutations in the α3(IV), α4(IV) or α5(IV) chains cause AS (15,18–20), which is characterized by glomerulonephritis combined with deafness and ocular abnormalities (12). To date, no missense mutations have been described in vertebrates in *Col4a1* or *Col4a2*. Heterozygous deficiency of *Col4a1*/*Col4a2* in mouse results in no apparent phenotype but complete absence induces early embryonic lethality (13). Mutations in the homologous collagen IV genes in *Caenorhabditis elegans* are embryonic lethal (21,22).

Here, we describe an allelic series of *Col4a1* point mutations that cause semi-dominant phenotypes in a number of tissues including eye and kidney. Homozygous *Bru* and *Raw* mutants are embryonic lethal; *Raw* homozygous mutants die by embryonic day 9.5. Mutant *Col4a1* mRNAs are expressed in these mutants, and we suggest that in heterozygotes, the mutant proteins act as dominant negative molecules and affect synthesis, secretion or function of the α1.α1.α2(IV) network. This network is expressed in many BMs and defects are found in kidney, eyes and other tissues such as oesophagus and aorta. The BM defects are local and include variable thinning, partial disintegration, rupturing and detachment from underlying cells. These primary defects cause secondary effects on cells and tissues such as glomerulopathy and ocular phenotypes.

Collagen molecules contain large domains characterized by Gly-Xaa-Yaa repeats in which the glycine residue is most critical for stable triple helix formation (reviewed in 23). In our allelic series, we observed a striking genotype–phenotype correlation between individual mutations. The *Raw* mutation affects the Yaa residue and results in a very subtle phenotype when compared with the *Svc* and *Bru* mutations, which affect glycine residues of the repeat. The severe mutations caused a more widespread pathology affecting BMs in multiple tissues. The different *Col4a1* mutant phenotypes are comparable with those seen in osteogenesis imperfecta where differences in severity are due to individual effects of the specific *COL1A1* or *COL1A2* mutations on chain association, triple helix formation, helix thermal stability and the different consequences when the mutant proteins are integrated in the extracellular fibres (24,25).

It remains to be determined how the mutant α1(IV) polypeptides result in the observed phenotypes. Mutant collagen IV in *C. elegans* is not secreted and leads to intracellular accumulation of unfolded collagen IV chains (21). This is also observed in ES cells deficient in HSP47, a protein involved in protomer formation in the ER in which the intracellular accumulation of collagen IV may trigger an apoptotic response (26). It is possible that the mutations in *Col4a1* prevent protein secretion by blocking assembly, helix formation or post-translational processing events. This is supported by the observed dilation

of the ER in the lens epithelium. If all collagen IV protomers containing a mutant α1(IV) chain were retained in the cell and/or degraded, there would simply be a reduction in the amount of protomer produced to 25% of WT.

Alternatively, some or all of the mutant protein may be secreted, may be incorporated in collagen IV networks and may alter the structure and interactive capacity of the collagen type IV network. This may compromise the stability and integrity of the BM or its formation and stable anchoring by disrupting interactions with other BM proteins or with matrix receptors, such as integrins or dystroglycan. This can be seen in local detachment of the matrix in epithelial BMs of *Bru* and *Raw* (Fig. 3). The more pronounced disruption of the BM in the areas between hemidesmosomes shows the effect of mutant collagen IV on cell–matrix interactions, as different integrin receptors, such as α3β1 integrin, are found in these regions. The presence of specific receptors such as α6β4 integrin in hemidesmosomes (27) may stabilize the BM sufficiently at these sites. A direct blocking of interactions with α1β1 and α2β1 integrins can be ruled out as the mutations are not located within the major binding site (28).

The phenotypes of the *Col4a1* mutants define a novel group of collagen IV defects unlike AS which is caused by defects in the α3.α4.α5(IV) network (12). Although both *Bru* mice and AS patients have kidney and eye pathologies, they are different. In AS, the GBM is mostly affected as mutations disrupt the α3.α4.α5(IV) network, which is crucial for the stability and function of the filtration barrier. Local degeneration of endothelial cells was observed in *Bru*, but no changes in podocytes are seen and the GBM appears to be unaffected. In contrast, Bowman's capsule is severely affected inducing epithelial hypertrophy, which is probably secondary. Lenticonus is observed in 25% of AS patients (29) but has not been observed in *Bru* mice, although both AS and *Bru* have cataracts (29,30). A missense mutation has been described in *COL4A4*, which leads to autosomal dominant AS combined with cholesterolaemia (31). Although the patients have typical GBM defects which are not observed in *Raw* and *Bru*, the arteriolar silvering in *Raw* could be explained by hypercholesterolaemia. Indeed, *Raw* males have a mild reduction in the levels of HDL cholesterol. However there was no reduction in females and both sexes display arteriolar silvering. In addition, histopathology did not reveal any evidence indicating that the silvery appearance in the retinal arterioles is caused by fat deposition. Finally, in contrast to AS patients who can have sensorineural deafness, no deafness was observed in the Raw and Svc mutants, which were tested using the SHIRPA protocols (32) (Pat Nolan, personal communication), and Bru, which was tested using a click test. Overall, these differences reflect the individual molecular defects caused by mutations in the α1.α1.α2(IV) or α3.α4.α5(IV) network.

Bru eyes show a number of potentially glaucoma-related phenotypes including iris/corneal adhesion, buphthalmos and optic nerve cupping. They also display iris defects, corneal opacity and cataracts. The combination of these eye phenotypes is similar to AR anomaly which includes iridocorneal adhesions, iris hypoplasia, eccentric pupil, corneal opaqueness and glaucoma (2). *Bru* may be a model for a syndrome similar to AR's anomaly, although so far no linkage has been reported of ASD to human chromosome 13q34, the location of *COL4A1*. However, it is worth noting that AR is genetically heterogeneous and a number of loci still remain to be identified (1,2).

The absence of abnormal histopathology underlines the subtlety of the *Raw* phenotype. However, ultrastructural analysis does reveal significant BM defects in some tissues, implying there is a threshold which has to be crossed before ultrastructural defects result in gross phenotypes and disrupt function. It is likely that the observed BM defects in retinal arterioles cause the arteriolar silvering, possibly by alterations in the reflective capacity of the vessel wall. The retinal arteriolar *Raw* phenotype, the BM defects in the retinal vessel wall and the bruising at birth in *Bru* and *Svc* animals strongly suggest that collagen type IV is important for vessel wall stability and vascular biology. During the revision of this manuscript, Gould *et al.* (33) showed that mutations in *Col4a1* lead to porencephaly. We have not observed porencephaly in our mutants. However, Gould *et al.* (33) allude to ocular and renal defects in their animals, although the nature of these is not specified.

In conclusion, the diverse consequences of *Col4a1* mutations described in this article define a spectrum of novel phenotypes, different from the loss of function mutation of *Col4a1/4a2*, which provides models for human disease pathologies.

MATERIALS AND METHODS

Animals

Studies were performed under guidance issued by the Medical Research Council and the UK Home Office.

Genome scan

A panel of 50 microsatellites (8) was amplified using DNA from 13 *Bru* mice. Primers were fluorescently labelled and analysed using ABI 310 Genetic Analyzer and ABI Genescan software (Applied Biosystems).

Identification of *Col4a1* mutations

The *Raw* and *Svc* mutations were identified by sequencing of exons. For *Bru*, both the cDNA and exons of *Col4a1* were sequenced. A list of primers is available upon request. RNA was isolated from *Bru* mice using Tri-Reagent (Sigma) and cDNA, generated using AMV Reverse-Transcriptase (Roche), was sequenced.

Phenotyping and histopathology

Bru eye phenotyping was performed using slit lamp examination as described earlier (http://www.eumorphia.org). Adult eyes and kidneys (3-month-old animals) were fixed overnight in Davidson's solution (eyes) and 4% PFA (kidney), respectively, and embedded in paraffin wax. Sections were stained with haematoxylin–eosin using standard protocols.

Urine samples were collected from three animals (5–6 months old). Gel loading buffer containing DTT was added

directly to urine samples and proteins were separated using 10% SDS–PAGE. Gels were stained using silver staining (Biorad). Protein content was determined using standard Bradford assay.

Ultrastructural analysis

Tissues were collected from three adult animals (3 months old) and fixed in 2.5% glutaraldehyde in 0.1 M phosphate buffer (pH 7.4) for 24 h at 4°C. After post-fixation in 1% buffered osmium tetroxide and standard processing for embedding in epoxy resin (EPON 812), tissues were analysed using transmission electron microscopy (LEO 906E, Oberkochen, Germany).

Immunohistochemistry

Cryosections were fixed for 10 min in acetone followed by antigen retrieval using 0.1 M HCl/KCl for 10 min. After blocking in PBS containing 10% FCS, sections were incubated with chain-specific rat monoclonal collagen IV antibodies (16), followed by incubation with FITC-conjugated secondary antibodies (Jackson Laboratories). Images were collected using a fixed exposure time.

ACKNOWLEDGEMENTS

We thank P. Gautier for bioinformatics assistance and expertise; N. Hastie and A. Hart for critical reading of the manuscript; Glaxo Smith Kline for financial support of the ENU mutagenesis screen. T.V.A. was supported by a Marie Curie Fellowship from the European Union and a Wellcome Trust Intermediate Research Fellowship. This work was supported by grants from the United Kingdom Medical Research Council (to I.J.J.).

Conflict of Interest statement. None declared.

REFERENCES

1. Gould, D.B. and John, S.W. (2002) Anterior segment dysgenesis and the developmental glaucomas are complex traits. *Hum. Mol. Genet.*, **11**, 1185–1193.
2. Lines, M.A., Kozlowski, K. and Walter, M.A. (2002) Molecular genetics of Axenfeld–Rieger malformations. *Hum. Mol. Genet.*, **11**, 1177–1184.
3. Mears, A.J., Jordan, T., Mirzayans, F., Dubois, S., Kume, T., Parlee, M., Ritch, R., Koop, B., Kuo, W.L., Collins, C. *et al.* (1998) Mutations of the forkhead/winged-helix gene, *FKHL7*, in patients with Axenfeld–Rieger anomaly. *Am. J. Hum. Genet.*, **63**, 1316–1328.
4. Nishimura, D.Y., Swiderski, R.E., Alward, W.L., Searby, C.C., Patil, S.R., Bennet, S.R., Kanis, A.B., Gastier, J.M., Stone, E.M. and Sheffield, V.C. (1998) The forkhead transcription factor gene *FKHL7* is responsible for glaucoma phenotypes which map to 6p25. *Nat. Genet.*, **19**, 140–147.
5. Semina, E.V., Reiter, R., Leysens, N.J., Alward, W.L., Small, K.W., Datson, N.A., Siegel-Bartelt, J., Bierke-Nelson, D., Bitoun, P., Zabel, B.U. *et al.* (1996) Cloning and characterization of a novel bicoid-related homeobox transcription factor gene, *RIEG*, involved in Rieger syndrome. *Nat. Genet.*, **14**, 392–399.
6. Alward, W.L., Semina, E.V., Kalenak, J.W., Heon, E., Sheth, B.P., Stone, E.M. and Murray, J.C. (1998) Autosomal dominant iris hypoplasia is caused by a mutation in the Rieger syndrome (*RIEG/PITX2*) gene. *Am. J. Ophthalmol.*, **125**, 98–100.
7. Justice, M.J., Noveroske, J.K., Weber, J.S., Zheng, B. and Bradley, A. (1999) Mouse ENU mutagenesis. *Hum. Mol. Genet.*, **8**, 1955–1963.
8. Thaung, C., West, K., Clark, B.J., McKie, L., Morgan, J.E., Arnold, K., Nolan, P.M., Peters, J., Hunter, A.J., Brown, S.D. *et al.* (2002) Novel ENU-induced eye mutations in the mouse: models for human eye disease. *Hum. Mol. Genet.*, **11**, 755–767.
9. Cattanach, B.M., Evans, E.P., Burtenshaw, M., Glenister, P.H., Vizor and Woodward (1993) Radiation-induced deletions. *Mouse Genome*, **91**, 853–854.
10. Lyon, M., Glenister, P.H. and West, J.D. (1984) Bruised (Bru). *Mouse News Lett.*, **71**, 26.
11. Khaw, P.T., Shah, P. and Elkington, A.R. (2004) Glaucoma-1: diagnosis. *BMJ*, **328**, 97–99.
12. Hudson, B.G., Tryggvason, K., Sundaramoorthy, M. and Neilson, E.G. (2003) Alport's syndrome, Goodpasture's syndrome, and type IV collagen. *N. Engl. J. Med.*, **348**, 2543–2556.
13. Poschl, E., Schlotzer-Schrehardt, U., Brachvogel, B., Saito, K., Ninomiya, Y. and Mayer, U. (2004) Collagen IV is essential for basement membrane stability but dispensable for initiation of its assembly during early development. *Development*, **131**, 1619–1628.
14. Kalluri, R., Shield, C.F., Todd, P., Hudson, B.G. and Neilson, E.G. (1997) Isoform switching of type IV collagen is developmentally arrested in X-linked Alport syndrome leading to increased susceptibility of renal basement membranes to endoproteolysis. *J. Clin. Invest.*, **99**, 2470–2478.
15. Sasaki, S., Zhou, B., Fan, W.W., Kim, Y., Barker, D.F., Denison, J.C., Atkin, C.L., Gregory, M.C., Zhou, J., Segal, Y. *et al.* (1998) Expression of mRNA for type IV collagen alpha1, alpha5 and alpha6 chains by cultured dermal fibroblasts from patients with X-linked Alport syndrome. *Matrix Biol.*, **17**, 279–291.
16. Sado, Y., Kagawa, M., Kishiro, Y., Sugihara, K., Naito, I., Seyer, J.M., Sugimoto, M., Oohashi, T. and Ninomiya, Y. (1995) Establishment by the rat lymph node method of epitope-defined monoclonal antibodies recognizing the six different alpha chains of human type IV collagen. *Histochem. Cell Biol.*, **104**, 267–275.
17. Kalluri, R. (2003) Basement membranes: structure, assembly and role in tumour angiogenesis. *Nat. Rev. Cancer*, **3**, 422–433.
18. Mochizuki, T., Lemmink, H.H., Mariyama, M., Antignac, C., Gubler, M.C., Pirson, Y., Verellen-Dumoulin, C., Chan, B., Schroder, C.H., Smeets, H.J. *et al.* (1994) Identification of mutations in the alpha 3(IV) and alpha 4(IV) collagen genes in autosomal recessive Alport syndrome. *Nat. Genet.*, **8**, 77–81.
19. Lemmink, H.H., Mochizuki, T., van den Heuvel, L.P., Schroder, C.H., Barrientos, A., Monnens, L.A., van Oost, B.A., Brunner, H.G., Reeders, S.T. and Smeets, H.J. (1994) Mutations in the type IV collagen alpha 3 (*COL4A3*) gene in autosomal recessive Alport syndrome. *Hum. Mol. Genet.*, **3**, 1269–1273.
20. Martin, P., Heiskari, N., Zhou, J., Leinonen, A., Tumelius, T., Hertz, J.M., Barker, D., Gregory, M., Atkin, C., Styrkarsdottir, U. *et al.* (1998) High mutation detection rate in the COL4A5 collagen gene in suspected Alport syndrome using PCR and direct DNA sequencing. *J. Am. Soc. Nephrol.*, **9**, 2291–2301.
21. Gupta, M.C., Graham, P.L. and Kramer, J.M. (1997) Characterization of alpha1(IV) collagen mutations in *Caenorhabditis elegans* and the effects of alpha1 and alpha2(IV) mutations on type IV collagen distribution. *J. Cell Biol.*, **137**, 1185–1196.
22. Sibley, M.H., Graham, P.L., von Mende, N. and Kramer, J.M. (1994) Mutations in the alpha 2(IV) basement membrane collagen gene of *Caenorhabditis elegans* produce phenotypes of differing severities. *EMBO J.*, **13**, 3278–3285.
23. Myllyharju, J. and Kivirikko, K.I. (2004) Collagens, modifying enzymes and their mutations in humans, flies and worms. *Trends Genet.*, **20**, 33–43.
24. Prockop, D.J., Constantinou, C.D., Dombrowski, K.E., Hojima, Y., Kadler, K.E., Kuivaniemi, H., Tromp, G. and Vogel, B.E. (1989) Type I procollagen: the gene–protein system that harbors most of the mutations causing osteogenesis imperfecta and probably more common heritable disorders of connective tissue. *Am. J. Med. Genet.*, **34**, 60–67.
25. Byers, P.H. (1989) Inherited disorders of collagen gene structure and expression. *Am. J. Med. Genet.*, **34**, 72–80.
26. Marutani, T., Yamamoto, A., Nagai, N., Kubota, H. and Nagata, K. (2004) Accumulation of type IV collagen in dilated ER leads to apoptosis in Hsp47-knockout mouse embryos via induction of CHOP. *J. Cell Sci.*, **117**, 5913–5922.
27. Nievers, M.G., Schaapveld, R.Q. and Sonnenberg, A. (1999) Biology and function of hemidesmosomes. *Matrix Biol.*, **18**, 5–17.

28. Eble, J.A., Golbik, R., Mann, K. and Kuhn, K. (1993) The alpha 1 beta 1 integrin recognition site of the basement membrane collagen molecule [alpha 1(IV)]2 alpha 2(IV). *EMBO J.*, **12**, 4795–4802.
29. Colville, D.J. and Savige, J. (1997) Alport syndrome. A review of the ocular manifestations. *Ophthalmic Genet.*, **18**, 161–173.
30. Streeten, B.W., Robinson, M.R., Wallace, R. and Jones, D.B. (1987) Lens capsule abnormalities in Alport's syndrome. *Arch. Ophthalmol.*, **105**, 1693–1697.
31. Ciccarese, M., Casu, D., Ki Wong, F., Faedda, R., Arvidsson, S., Tonolo, G., Luthman, H. and Satta, A. (2001) Identification of a new mutation in the alpha4(IV) collagen gene in a family with autosomal dominant Alport syndrome and hypercholesterolaemia. *Nephrol. Dial. Transplant.*, **16**, 2008–2012.
32. Rogers, D.C., Fisher, E.M., Brown, S.D., Peters, J., Hunter, A.J. and Martin, J.E. (1997) Behavioral and functional analysis of mouse phenotype: SHIRPA, a proposed protocol for comprehensive phenotype assessment. *Mamm. Genome.*, **8**, 711–713.
33. Gould, D.B., Phalan, F.C., Breedveld, G.J., van Mil, S.E., Smith, R.S., Schimenti, J.C., Aguglia, U., van der Knaap, M.S., Heutink, P. and John, S.W. (2005) Mutations in Col4a1 cause perinatal cerebral hemorrhage and porencephaly. *Science*, **308**, 1167–1171.